Article

Aqueous Ligand-Stabilized Palladium Nanoparticle Catalysts for Parahydrogen Induced 13C Hyperpolarization

Jeffrey McCormick, Alexander M. Grunfeld, Yavuz N. Ertas, Akash Neil Biswas, Kristofer Lee Marsh, Shawn Wagner, Stefan Gloggler, and Louis-S. Bouchard

Anal. Chem., **Just Accepted Manuscript** • Publication Date (Web): 07 Jun 2017

Aqueous Ligand-Stabilized Palladium Nanoparticle Catalysts for Parahydrogen Induced ^{13}C Hyperpolarization

Jeffrey McCormick[a.b], Alexander M. Grunfeld[a], Yavuz N. Ertas[b,c], Akash N. Biswas[a], Kristofer L. Marsh[a], Shawn Wagner[d], Stefan Glöggler[a,e,f], Louis-S. Bouchard*[a,b,c]

[a]Department of Chemistry and Biochemistry, University of California at Los Angeles, 607 Charles E Young Drive East, Los Angeles, CA 90095-1569, USA

[b]The Molecular Biology Institute, Jonsson Comprehensive Cancer Center, California NanoSystems Institute (CNSI), University of California Los Angeles, Los Angeles, CA 90095, USA

[c]Department of Bioengineering, University of California at Los Angeles, 420 Westwood Plaza, Los Angeles, CA 90095, USA

[d]Biomedical Imaging Research Institute, Cedars Sinai Medical Center, 8700 Beverly Blvd, Davis Building G149E, Los Angeles, CA 90048, USA

[e]Max Planck Institute for Biophysical Chemistry, Am Fassberg 11, D-37077 Göttingen, Germany

[f]Center for Biostructural Imaging of Neurodegeneration, Von-Siebold-Str. 3A, D-37075 Göttingen, Germany

Keywords: parahydrogen induced polarization • palladium nanoparticles • heterogeneous catalysis • polarization transfer • hyperpolarization

ABSTRACT: Parahydrogen induced polarization (PHIP) is a method for enhancing NMR sensitivity. The pairwise addition of parahydrogen in aqueous media by heterogeneous catalysts can lead to applications in chemical and biological systems. Polarization enhancement can be transferred from ^{1}H to ^{13}C for longer lifetimes by use of zero field cycling. In this work, water-dispersible N-acetylcysteine- and L-cysteine-stabilized palladium nanoparticles are introduced and carbon polarizations up to two orders of magnitude higher than previous aqueous heterogeneous PHIP systems are presented. P_{13C} values of 1.2% and 0.2% are achieved for the formation of hydroxyethyl propionate from hydroxyethyl acrylate and ethyl acetate from vinyl acetate, respectively. Both nanoparticle systems are easily synthesized in open air, and TEM indicates an average size of 2.4 ± 0.6 nm for NAC@Pd and 2.5 ± 0.8 nm for LCys@Pd nanoparticles with 40% and 25% ligand coverage determined by thermogravimetric analysis, respectively. As a step toward biological relevance, results are presented for the unprotected amino acid allylglycine upon aqueous hydrogenation of propargylglycine.

Introduction

Although prevalent in chemical, biological and biomedical sciences, nuclear magnetic resonance (NMR) suffers from inherently low sensitivity due to the constraints of thermal polarization of nuclear spins at liquid water temperatures. The advent of hyperpolarization methods such as dynamic nuclear polarization (DNP)[1,2], parahydrogen-induced polarization (PHIP)[3] and signal amplification by reversible exchange (SABRE)[4–6] has led to enhancements of detectable magnetization by several orders of magnitude[7].

Dissolution DNP, a technique involving the transfer of polarization from unpaired electrons to nuclear spins at near absolute zero temperature, has recently been applied *in vivo*[8]. While DNP has been demonstrated in biomedical applications, current DNP methods are limited by long polarization times and costly equipment. SABRE and PHIP techniques utilize the *para* nuclear spin isomer, parahydrogen (para-H_2). Para-H_2 is generated by passing hydrogen gas over a catalyst bed at low temperature. At 20 K, the purity of the para-H_2 spin state can be enriched to as high as 99.82%[9], and is stable when pressurized and stored at room temperature. The subsequent polarization enhancement of para-H_2 is then obtained by hydrogenation of unsaturated precursors during PHIP, or non-hydrogenative coordination via SABRE.

Current PHIP methods predominantly use homogeneous transition metal catalysts such as $[Rh(I)(nbd)_2]^+[BF_4]^-$ and its derivatives[10,11]. The homogeneous catalyst cannot be readily removed from the mixture, which raises toxicity concerns due to the high metal concentration. To overcome this clinically limiting challenge, aqueous heterogeneous platinum catalysts have recently been demonstrat-

ed to achieve ^{1}H polarization values as high as 0.7%[12,13], near the threshold for biological consideration ($P_{1H} \geq 1\%$)[14]. Phase separation techniques of soluble catalysts have been demonstrated using 2-propynyl-2-oxopropanoate hydrogenation into pyruvate before aqueous extraction; however, this method resulted in ~40% reduction of hyperpolarized product as well as additional signal loss from relaxation[15]. Unlike homogeneous catalysts, heterogeneous catalysts have the potential to be immobilized on support material allowing for quick filtration of the catalyst away from the hyperpolarized molecules in solution, a necessary requirement for potential clinical utilization.

In this work, ligand-stabilized palladium nanoparticles are introduced and characterized as water-soluble catalysts demonstrating the highest heterogeneous carbon and proton polarizations to date (P_{13C} = 1.2%, P_{1H} = 1.2%) in water, in nearly identical conditions to previous experiments using a water-optimized homogenous Rh catalyst[11]. The cost of palladium per gram is significantly lower than that of platinum, making this type of catalyst attractive. Comparison of nanoparticle synthesis methods and surface oxidation under inert conditions versus open air shows that air-synthesized nanoparticles retain equivalent polarization ability, granting higher polarization performance in lower-cost, simple synthesis conditions.

Two particle-capping amino acid ligands are investigated herein: L-cysteine (LCys), and its analog, N-acetylcysteine (NAC). Both ligands are biologically compatible small molecules shown to coordinate strongly to transition metals and create stable, water-soluble nanoparticles[13]. Because ^{1}H relaxation times are short-lived (T_1 of usually ≤ 1 s), *in vivo* applications likely hinge on the preservation of hyperpolarized state by transfer of polarization to nearby heteronuclei with longer relaxation times such as ^{13}C.

Heterogeneous PHIP has been demonstrated in gas phase reactions[16,17], and has recently been shown in water[18] at P_{13C} ~0.01%. The present work demonstrates two orders of magnitude improvement, as well as potential for ligand optimization rather than bare metal systems. To demonstrate the potential for biological applications, the acetate precursor ethyl acetate (EA) is hyperpolarized from vinyl acetate (VA), a compound previously shown in PHIP side arm hydrogenation (PHIP-SAH) investigations[15]. Acetate is a relevant metabolite for *in vivo* hyperpolarization studies[19]. Hyperpolarized hydroxyethyl propionate (HEP), a compound previously demonstrated in *in vivo* angiography[20], is also shown by hydrogenation of 2-hydroxyethyl acrylate (HEA).

Transfer of polarization from para-H_2 to adjacent ^{13}C is achieved by cycling hydrogenation product mixtures in and out of zero field using a concentric ring μ-metal chamber. The amino acid propargylglycine (PraH) is parahydrogenated into hyperpolarized allylglycine without chemical protection on the amine, and ^{1}H polarization of P_{1H} = 0.9% is shown. This is the first demonstration of aqueous PHIP of an unprotected amino acid by a heterogeneous catalyst.

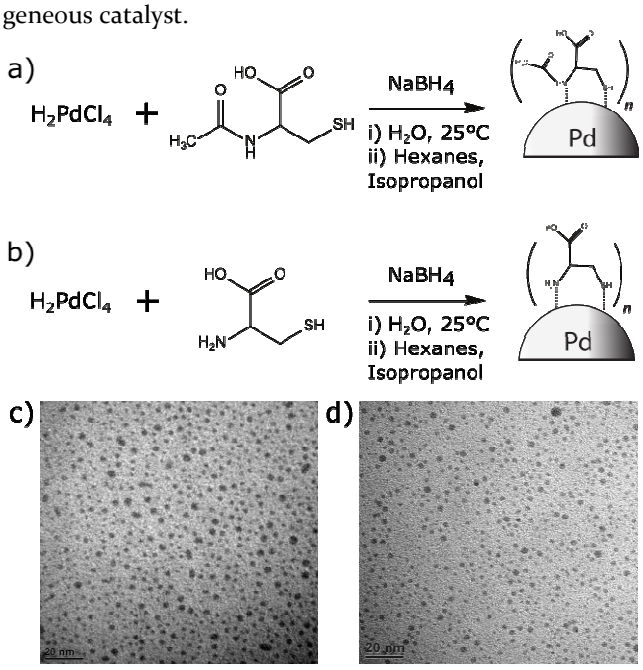

Figure 1. Synthesis summaries of a) NAC@Pd and b) LCys@Pd nanoparticles. TEM shows an average particle size of c) 2.4 ± 0.6 nm for NAC@Pd, and d) 2.5 ± 0.8 nm for LCys@Pd.

Experimental Section

Figure 1a) and 1b) show the synthesis schemes of NAC@Pd and LCys@Pd, respectively. For both systems, the precursor H_2PdCl_4 was dissolved in water and reduced by $NaBH_4$ in the presence of ligand at a molar ratio of 1:1 in open air.

Solvent fractionation using isopropanol and hexanes followed by centrifugation and repeated washes with ethanol yielded nanoparticle products stored after drying. TEM images of LCys@Pd and NAC@Pd prepared in water shown in Fig 1c) and d) reveal average particle sizes of 2.5 ± 0.8 nm and 2.4 ± 0.6 nm, respectively (see Fig. S3 for sizing details). UV/Vis and X-ray photoelectron spectroscopy (XPS) reveal Pd^0 nanoparticle formation and higher Pd-O surface oxidation during air synthesis (see Fig. S6). PHIP experiments were performed as previously described[12,13] and the resulting spectra are shown in Figure 2. Nanoparticles and substrate were suspended in degassed D_2O and heated to 80°C before pressurization with para-H_2 to 6.5 bar. The sample was shaken in transit to the magnet and inserted for ^{1}H experiments whereas for ^{13}C a field cycling step was included before scanning. The data was acquired after a single 45°$_x$ (^{1}H) or 90°$_x$ (^{13}C) pulse, and the enhancement calculated by comparison to thermal spectra. Concentration experiments showed optimal polarization of P_{1H} = 1.2% at 10 mg/mL for both nanoparticles (see Fig. S7).

Discussion

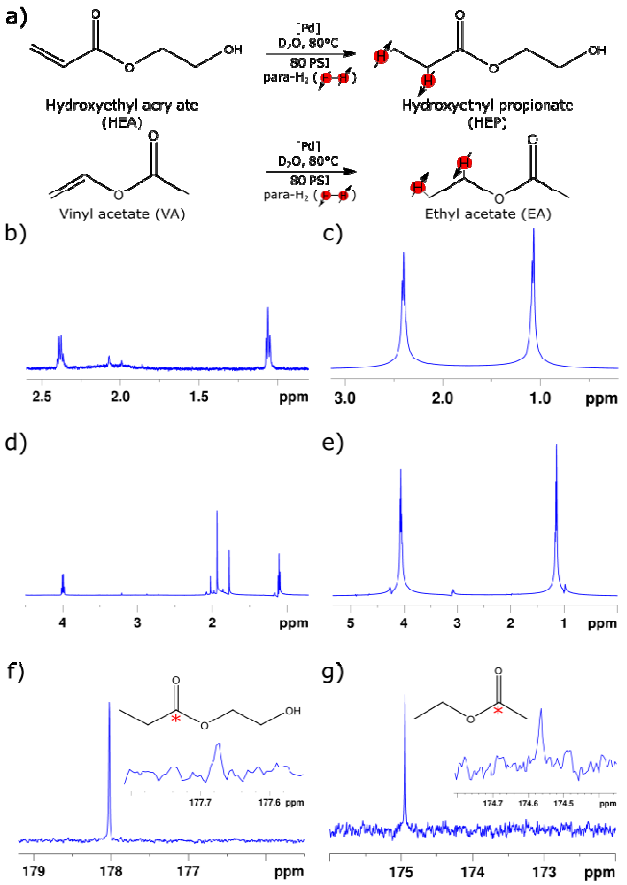

Figure 2. a) Reaction mechanism of VA and HEA hydrogenation and transfer of polarization to ^{13}C. Thermal ^{1}H spectra of b) HEP and d) EA, as well as their hyperpolarized spectra (c) and e), respectively. ^{13}C hyperpolarized spectra following zero field transfer for f) HEA and g) EA products with thermal spectra overlaid are also shown. Thermal ^{13}C spectra were acquired after 256 scans. Spectra shown in magnitude mode.

In heterogeneous PHIP, pairwise addition of para-H_2 is thought to be preserved by ligand density, which limits diffusion across the particle surface. Significant diffusion would otherwise lead to loss of para-H_2 spin order[12]. Thus, ligands are chosen not only for control of particle disperse sity and solubility, but also for their ability to restrict H_2 diffusion (and catalytic exchange between hydrogen molecules) during hydrogenation reactions. LCys and NAC were selected for this work based on biocompatibility, convenient thiol and amine groups involved in transition metal coordination, and previous demonstration of heterogeneous PHIP in platinum nanoparticle systems[12,13].

Previous studies have proposed NAC as a control experiment in which amine coordination is blocked and thus limiting surface diffusion[13]. However, coordination of nitrogen on NAC is not blocked and serves to stabilize Pt and Pd nanoparticles tightly enough to produce recyclable particles in this work (see S8 in SI) and elsewhere[13]. Au nanoparticles have been recently demonstrated as sensitive colorimetric probes for the detection of NAC due to strong functional group interaction[21], supporting this interpretation.

This suggests a strong geometric dependence on ligand involvement in pairwise hydrogenation as LCys and NAC are similar in size, yet undergo different binding mechanisms due to amine protection, which may orient NAC in a more favorable position for pairwise addition on the Pd surface. Consistent synthesis procedures also showed NAC@Pd ligand density 1.6x higher than that of LCys@Pd, despite similar particle size (40%wt versus 25%wt, Table 1). This increase cannot be explained solely by the difference in molecular weight of NAC compared to LCys (163.19 versus 121.16 g/mol, respectively). This suggests that NAC is better able to stack on the particle surface, and that this efficient stacking contributes to the ability of NAC to improve pairwise H_2 addition. Nanoparticle fractionation demonstrated higher polarization than the bulk nanoparticle mixture (data not shown). Previous work has reported lower ligand densities for Pt nanoparticle systems without solvent fractionation[12,13].

Due to Pd nanoparticles' tendency to crystallize in the fcc structure[22] and TEM confirming spherical geometry, a cubo-octahedral structure can be assumed in turnover frequency (TOF) calculations[23]. TOF calculations were performed by flowing H_2 into nanoparticle mixtures with HEA under ambient N_2 flow heated to 80° C and conversion was monitored by NMR every 15 minutes to compare catalyst activity. Often, high ligand coverage of a catalytic surface sacrifices activity due to reduction of available catalytic sites, yet surprisingly NAC@Pd showed a TOF of 1.97x that of LCys@Pd despite higher ligand density (Ta-

Table 1. Summary of nanoparticle characteristics.

Nanoparticle	Diameter (nm)	Ligand Density (%wt)	^{1}H Polarization, HEP (%P)	^{1}H Polarization, PraH (%P)	^{13}C Polarization, HEP (%P)	^{13}C Polarization, EA (%P)	Ligands (mmol/g)	Surface Area (m2/mg)	TOF (h-1)
NAC@Pd	2.4 ± 0.6	40	1.2 ± 0.1	0.9 ± 0.2	1.2 ± 0.1	0.20 ± 0.03	2.45	1.81 x 10-10	42.9
LCys@Pd	2.5 ± 0.8	25	0.9 ± 0.1	-	-	-	2.06	1.96 x 10-10	21.7

ble 1). This work utilizing the catalyst NAC@Pd demonstrates nanoparticle systems showing 1.71x higher ^{1}H polarization and 1.35x higher TOF than was previously shown with Pt nanoparticles of similar diameter[13]. The current catalyst NAC@Pd TOF corresponds to production of 1.1 μmol of HEP product in the 10 s time period following parahydrogenation, resulting in 1.1 mM in 1 mL solution. This conversion is also measured at ambient pressure H_2, far lower than PHIP experimental conditions (6.5 bar para-H_2). Recently, work by Zacharias *et al*[14] demonstrates metabolic imaging of hyperpolarized aqueous diethyl succinate. Soluble Rh(dppb)(nbd)BF_4 catalyst was dissolved and used to hydrogenate diethyl fumarate (20 mM) before injection into live mice using an optimized polarizer and deuterated compounds for spin preservation. Comparison with our system indicates our current catalyst is a mere 18-fold concentration and 2-fold polarization away from current *in vivo* investigations. Considering that 1.1 mM is typical for most physiological conditions, the catalyst systems proposed here may be sufficient for *in vivo* use. Since transit time to the magnet was recorded at 9 seconds from pressurization to spectra acquisition, it is possible that with a well-optimized polarizer nearly two full T_1 relaxation cycles[13] could be avoided, leading to potential polarizations ≥ 10%.

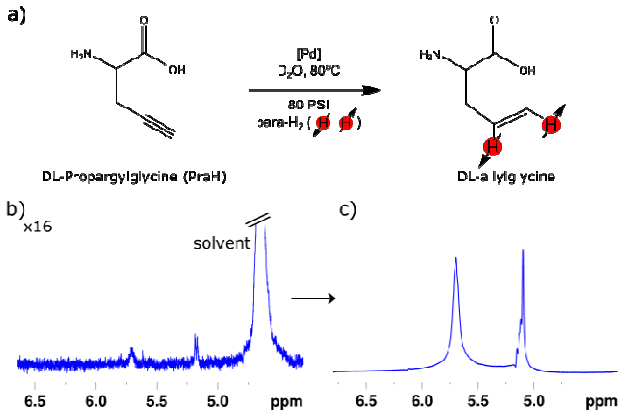

Figure 3. a) PHIP mechanism of propargylglycine into allylglycine. b) Thermal and c) hyperpolarized ^{1}H spectra of allyglycine peaks following hydrogenation. Spectra shown in magnitude mode.

As advances in PHIP are made towards broader investigation of biologically relevant substrates, one barrier is that unprotected functional groups have been shown to hinder polarization due to unfavorable interactions with PHIP catalysts[11,24]. Because of this problem and widespread interest in hyperpolarized peptides, protecting groups for amines and carboxylates are often investigated to create product analogs of varying biological activity and solubility. Strategies proposed to remove the protecting group by cleavage after para-H_2 addition[15] are untenable for a clinically relevant technique. In this work, aqueous parahydrogenation of unprotected DL-propargylglycine is investigated as a substrate for NAC@Pd to demonstrate the advantage in using a heterogeneous system. Propargylglycine (PraH) is a naturally occurring, water-soluble amino acid found in certain fungal systems[25] with an unsaturated triple bond. ^{1}H PHIP experiments using Boc-protected PraH in methanol-d_4 and homogeneous Rh(dppb)(COD)BF_4 catalyst yielded polarization values of P_{1H} = 0.4%, comparable to ~1.2% when adjusting from 50% para-H_2 enrichment to ~100%[26]. PraH has recently been incorporated into sunflower typsin inhibitor along with O-propargyl-L-tyrosine in mixed solvent system to yield P_{1H} = 0.14% (expected 0.42% with ~100% para-H_2) without loss of activity[27], demonstrating PraH's potential in biological investigations.

Figure 3 shows hyperpolarized ^{1}H peaks from DL-allylglycine, yielding a polarization of P_{1H} = 0.9%. However, PraH's triple bond has the potential for two parahydrogenations[14], allowing further enhancement under higher conversion regimes, though only characteristic I_z–S_z peaks for allylglycine are observed here. Both investigations of propyne in gas-phase heterogeneous PHIP[28] and O-propargyl-L-tyrosine in solution PHIP[27] report only single hydrogenation product enhancement. Magnetic field cycling experiments were attempted on PraH, though no ^{13}C enhancement was observed. This can be explained due to allylglycine's dense proton environment on adjacent carbons to the hydrogenation site which likely interfere with the observed magnetization after transfer. The relatively large distance to the ester carbon often chosen in ^{13}C transfer requires zero field draw speeds longer than para-H_2 relaxation and is unlikely to be observed.

In conclusion, this work demonstrates novel water-soluble palladium nanoparticles as catalysts in aqueous heterogeneous PHIP, capable of transferring polarization to ^{13}C on biologically relevant compounds. Both ^{13}C and ^{1}H polarizations are unprecedented in aqueous heterogeneous reactions, ^{13}C by up to two orders of magnitude compared to the previous state-of-the-art experiments. High ^{13}C enhancement on compounds of biological interest represents a crucial advancement in heterogeneous PHIP application. Similarly, robust polarization of unprotected peptides and other nitrogenous compounds widens the breadth of potential PHIP labels to meet the future needs of diagnostic imaging.

ASSOCIATED CONTENT

Supporting Information. Materials and Methods, Synthetic Procedures, Nanoparticle Characterization, PHIP Experiments, Nanoparticle Recovery. This material is available free of charge via the Internet at http://pubs.acs.org.

AUTHOR INFORMATION

Corresponding Author

*Professor Louis Bouchard
louis.bouchard@gmail.com

Present Addresses

†If an author's address is different than the one given in the affiliation line, this information may be included here.

Author Contributions

All authors have given approval to the final version of the manuscript.

Funding Sources

The authors would like to gratefully acknowledge financial support from the National Science Foundation (NSF) (research grants CHE-1153159, CHE-1508707, equipment grant CHE-1048804), the Arnold and Mabel Beckman Foundation, The Max Planck Society and the Jonsson Comprehensive Cancer Center Foundation at UCLA.

ABBREVIATIONS

PHIP, parahydrogen-induced polarization; Pd, palladium; NMR, nuclear magnetic resonance; PraH, propargylglycine; LCys, L-cysteine; TEM, Transmission Electron Microscopy; NAC, N-acetylcysteine; .

REFERENCES

(1) Gallagher, F. A.; Kettunen, M. I.; Day, S. E.; Hu, D.-E.; Ardenkjær-Larsen, J. H.; Zandt, R. in 't; Jensen, P. R.; Karlsson, M.; Golman, K.; Lerche, M. H.; Brindle, K. M. *Nature* **2008**, *453* (7197), 940–943.

(2) Ardenkjaer-Larsen, J. H.; Fridlund, B.; Gram, A.; Hansson, G.; Hansson, L.; Lerche, M. H.; Servin, R.; Thaning, M.; Golman, K. *Proc. Natl. Acad. Sci. U. S. A.* **2003**, *100* (18), 10158–10163.

(3) Bowers, C. R.; Weitekamp, D. P. *J. Am. Chem. Soc.* **1987**, *109* (18), 5541–5542.

(4) Adams, R. W.; Aguilar, J. A.; Atkinson, K. D.; Cowley, M. J.; Elliott, P. I. P.; Duckett, S. B.; Green, G. G. R.; Khazal, I. G.; López-Serrano, J.; Williamson, D. C. *Science.* **2009**, *323* (80), 1708–1711.

(5) Theis, T.; Truong, M. L.; Coffey, A. M.; Shchepin, R. V.; Waddell, K. W.; Shi, F.; Goodson, B. M.; Warren, W. S.; Chekmenev, E. Y. *J. Am. Chem. Soc.* **2015**, *137* (4), 1404–1407.

(6) Truong, M. L.; Shi, F.; He, P.; Yuan, B.; Plunkett, K. N.; Coffey, A. M.; Shchepin, R. V.; Barskiy, D. A.; Kovtunov, K. V.; Koptyug, I. V.; Waddell, K. W.; Goodson, B. M.; Chekmenev, E. Y. *J. Phys. Chem. B* **2014**, *118* (48), 13882–13889.

(7) Shchepin, R. V.; Coffey, A. M.; Waddell, K. W.; Chekmenev, E. Y. *Anal. Chem.* **2014**, *86* (12), 5601–5605.

(8) Koelsch, B. L.; Reed, G. D.; Keshari, K. R.; Chaumeil, M. M.; Bok, R.; Ronen, S. M.; Vigneron, D. B.; Kurhanewicz, J.; Larson, P. E. Z. *Magn. Reson. Med.* **2015**, *74* (3), 622–633.

(9) Svadlenak, R. The Ortho-Para Hydrogen Conversion on Iron Oxide-Zinc Oxide Catalysts, Oregon State College, 1955.

(10) Shchepin, R. V.; Coffey, A. M.; Waddell, K. W.; Chekmenev, E. Y. *J. Phys. Chem. Lett.* **2012**, *3* (22), 3281–3285.

(11) Gloggler, S.; Wagner, S.; Bouchard, L.-S. *Chem. Sci.* **2015**.

(12) Glöggler, S.; Grunfeld, A. M.; Ertas, Y. N.; McCormick, J.; Wagner, S.; Schleker, P. P. M.; Bouchard, L. S. *Angew. Chemie - Int. Ed.* **2015**, *54* (8), 2452–2456.

(13) Gloggler, S.; Grunfeld, A. M.; Ertas, Y. N.; McCormick, J.; Wagner, S.; Bouchard, L. S. *Chem. Commun.* **2016**, *52* (3), 605–608.

(14) Zacharias, N. M.; Chan, H. R.; Sailasuta, N.; Ross, B. D.; Bhattacharya, P. *J. Am. Chem. Soc.* **2012**, *134*, 934–943.

(15) Reineri, F.; Boi, T.; Aime, S. *Nat. Commun.* **2015**, *6*, 5858.

(16) Bouchard, L. S.; Kovtunov, K. V.; Burt, S. R.; Anwar, M. S.; Koptyug, I. V.; Sagdeev, R. Z.; Pines, A. *Angew. Chemie - Int. Ed.* **2007**, *46* (22), 4064–4068.

(17) Bouchard, L.-S.; Burt, S. R.; Anwar, M. S.; Kovtunov, K. V.; Koptyug, I. V.; Pines, A. *Science (80-.).* **2008**, *319* (5862), 442–445.

(18) Kovtunov, K. V.; Barskiy, D. A.; Shchepin, R. V.; Salnikov, O. G.; Prosvirin, I. P.; Bukhtiyarov, A. V.; Kovtunova, L. M.; Bukhtiyarov, V. I.; Koptyug, I. V.; Chekmenev, E. Y. *Chem. - A Eur. J.* **2016**, *22* (46), 16446–16449.

(19) Bastiaansen, J. A. M.; Cheng, T.; Mishkovsky, M.; Duarte, J. M. N.; Comment, A.; Gruetter, R. *Biochim. Biophys. Acta - Gen. Subj.* **2013**, *1830* (8), 4171–4178.

(20) Bhattacharya, P.; Harris, K.; Lin, A. P.; Mansson, M.; Norton, V. A.; Perman, W. H.; Weitekamp, D. P.; Ross, B. D. *Magn. Reson. Mater. Physics, Biol. Med.* **2005**, *18* (5), 245–256.

(21) Rastegarzadeh, S.; Hashemi, F. *Anal. Methods* **2015**, *7*, 1478–1483.

(22) Sharma, S.; Kim, B.; Lee, D. *Langmuir* **2012**, *28* (45), 15958–15965.

(23) Hardeveld, R. V. A. N.; Hartog, F. *Surf. Sci.* **1969**, *15*, 189–230.

(24) Gruppi, F.; Xu, X.; Zhang, B.; Tang, J. A.; Jerschow, A.; Canary, J. W. *Angew. Chemie - Int. Ed.* **2012**, *51* (47), 11787–11790.

(25) A Kawaji, K Yamauchi, S Fujii, R Natsuki, E Takabatake, Y. Y. *J. Pharmacobiodyn.* **1992**, *15* (3), 107–112.

(26) Körner, M.; Sauer, G.; Heil, A.; Nasu, D.; Tietze, D.; Voigt, S.; Weidler, H.; Gutmann, T.; Avrutina, O.; Kolmar, H.; Ratajczyk, T.; Buntkowsky, G. *Chem. Commun.* **2013**, 7839–7841.

(27) Sauer, G.; Nasu, D.; Tietze, D.; Gutmann, T.; Englert, S.; Avrutina, O.; Kolmar, H.; Buntkowsky, G. *Angew. Chemie - Int. Ed.* **2014**, *53* (47), 12941–12945.

(28) Kovtunov, K. V.; Zhivonitko, V. V.; Corma, A.; Koptyug, I. V. *J. Phys. Chem. Lett.* **2010**, *1* (11), 1705–1708.

TOC Artwork: